Enhancement of electronic conductivity of $LiFePO_4$ by Cr doping and its identification by first-principles calculations

Siqi Shi, Lijun Liu, Chuying Ouyang, Ding-sheng Wang, Zhaoxiang Wang, Liquan Chen, and Xuejie Huang
Institute of Physics, Chinese Academy of Sciences, P.O. Box 603, Beijing, 100080, China
(Received 25 July 2003; published 11 November 2003)

We present a first-principles electronic band structure for pure $LiFePO_4$, delithiated $FePO_4$, and Cr-doped $LiFePO_4$. It indicates that not only Fe but also O atoms are oxidized in the delithiation process, while P is little affected. This is in contrast to the usual view of the intercalation reaction that the removal of Li only transforms Fe from Fe^{2+} to Fe^{3+}, but in agreement with the present x-ray photoemission spectroscopy experiment. Calculation also assumes a significant enhancement of electronic conductivity when lithium ions are replaced by cations with higher valence, Cr^{3+}. We also confirm experimentally, for $Li_{1-3x}Cr_xFePO_4$ with $x=0.01$ and 0.03, an enhancement of the electronic conductivity up to eight orders of magnitude comparing with pure $LiFePO_4$. Besides the conventional *p*-type doping conductivity, another mechanism has been suggested, which involves the electron hopping within a cluster surrounding the doping atom and related vacancies, and electron tunneling between these conducting clusters.

DOI: 10.1103/PhysRevB.68.195108 PACS number(s): 72.20.−i, 61.72.−y, 71.22.+i, 84.60.−h

The need for high energy density rechargeable batteries for portable electronic devices, electrical vehicles, and dispersed-type energy storage systems has led to the development of lithium ion battery experimentally and theoretically.[1–4] The performance of lithium ion batteries depends strongly on the properties of related materials, and many kinds of materials have been investigated as the cathode materials for lithium ion batteries.[5] Recently, iron-based compound containing compact tetrahedral ''polyanion'' structural units $(XO_4)^{n-}$ (X=S, P, As, W, or Mo) have been investigated intensively as potential cathode materials for lithium ion batteries.[6–9] The elements in the compounds are abundant in the earth, inexpensive, and environment friendly. Especially, orthorhombic $LiFePO_4$, which has an ordered olivine structure as shown in Fig. 1, has attracted most attention. However, it is generally accepted that this kind of compound is a semiconductor and has an extremely low electronic conductivity at room temperature. Various material processing approaches have been adopted to overcome this drawback, for example, Huang *et al.*[10] added conductive carbon into the nanocomposites of $LiFePO_4$ to achieve a better conductivity and thus improve the performance of the battery charging. But this is not an intrinsic enhancement of the bulk electronic conductivity of $LiFePO_4$, and the energy storage density has been reduced by the addition of carbon black. Surprisingly, Chung *et al.*[6] found that controlled cation nonstoichiometry combined with solid-solution doping by metals supervalent to Li^+, e.g., Mg, Zr, and Nb, increases the electronic conductivity of $LiFePO_4$ by a factor of $\sim 10^8$. However, a controversy[11] exists with respect to the physical mechanism, that the olivine powders are synthesized from carbon-containing precursors such as carbonates, oxalates, and alkoxides with the result that, after firing under nitrogen or argon, the products contained residual carbon, by as much as 1.5% by weight. Therefore, the competitors thought it is not the doped supervalent metal but carbon that contributes significantly to electronic conductivity.

In this paper, the first-principles calculation, which has already made an impact on the understanding of practical lithium-ion batteries materials,[1,12–17] is used for pure $LiFePO_4$ and its delithiated counterpart $FePO_4$. It is found that not only Fe but also O are oxidized in the delithiation process. This is in contrast to the usual view, but in agreement with the present x-ray photoemission spectroscopy experiment.[18] Experimentally, a doping system has been studied by Goñi *et al.*,[19] who found that Fe^{3+} can substitute part of the Li^+ ions of $LiMgPO_4$ structure to form the solid solution $Li_{1-3x}Fe_xMgPO_4(0<x<0.1)$, creating cation vacancy channels along certain crystallographic direction. Similarly, Chung *et al.*[6] also noticed that a net cation deficiency occurs to Li ions upon such supervalent doping. Just based on this experimental illumination, the electronic structure of Cr doped $LiFePO_4$, namely, $Li_{1-3x}Cr_xFePO_4$ with $x=1/32$, has been calculated from first-principles in this paper in order to elucidate the underlying conducting mechanism. Following this theoretical calculation, we also fabricated and measured experimentally the Cr-doped $LiFePO_4$ samples, and found that its conductivity has been enhanced by substituting small amount of lithium ions, and the conducting mechanism has been discussed in light of our first-principles band calculation.

The calculation was performed using the Vienna *ab initio* simulation program, VASP.[20] We used the Vanderbilt ultrasoft

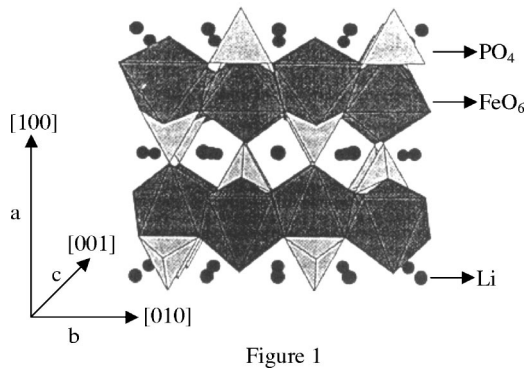

Figure 1

FIG. 1. Schematic drawing of the crystal structure of $LiFePO_4$.

TABLE I. Lattice parameters of $LiFePO_4$ and $FePO_4$. Atomic coordinates are given in units (a, b, and c).

	$LiFePO_4$ (Calc.)	$LiFePO_4$ (Expt. [a])	$FePO_4$ (Calc.)
a(Å)	10.487	10.332	10.382
b(Å)	5.915	6.011	5.986
c(Å)	4.748	4.692	4.710
V(Å^3)	294.521	291.400	292.711
Li ($4a$)	(0, 0, 0)	(0, 0, 0)	–
Fe ($4c$)	(0.282,0.25,0.975)	(0.280,0.25,0.991)	(0.284,0.25,0.989)
P ($4c$)	(0.095,0.25,0.418)	(0.095,0.25,0.420)	(0.094,0.25,0.416)
O_1 ($4c$)	(0.097,0.25,0.743)	(0.095,0.25,0.751)	(0.091,0.25,0.754)
O_2 ($4c$)	(0.457,0.25,0.206)	(0.449,0.25,0.209)	(0.458,0.25,0.209)
O_3 ($8d$)	(0.166,0.046,0.285)	(0.169,0.046,0.280)	(0.164,0.044,0.288)

[a]Ref. 24.

pseudopotential[21] and the generalized gradient approximation by Perdew and Wang (PW91) (Ref. 22) for the exchange-correlation energy. Since the non-spin-polarization calculation (see Figs. 3 and 4) has shown that pure LiFePO4 is a semiconductor, only performing the non-spin-polarization calculation is enough to meet the purpose of the present work. Besides the calculation carried out by the 28-atom orthorhombic $LiFePO_4$ unit cell and the delithiated $FePO_4$ unit cell, calculation for the undoped $LiFePO_4$ case has also been done by $2\times2\times2$ expanded supercell to bring comparison with the doped case described below. The total energy was converged to better than 2 meV per atom with a plane wave cutoff of 520 eV. When using a 28-atom unit cell for the case of pure $LiFePO_4$, 60 k points in the first Brillouin zone were used. The ionic positions, lattice parameters, and cell volume are all relaxed with the conjugated gradient method using forces and stresses. Fermi level is smeared by the Methfessel-Paxton[23] approach with a Gaussian width of 0.2 eV. The optimization was stopped when forces on all relaxed atoms were less than 0.03 eV/Å , which is accurate enough to ensure that the maximum displacement error is within 0.1 Å.

The optimized crystal parameters for $LiFePO_4$ and $FePO_4$ are listed in Table I, together with the experimental values of $LiFePO_4$. The calculated volume of the unit cell is only 1% larger than the experimental values for $LiFePO_4$. The computed Wyckoff coordinates are also in good agreement with experimental values. It is interesting to note that the lattice parameters, and the Fe-O and P-O bond lengths of $FePO_4$ change very slightly compared with $LiFePO_4$: Three lattice parameters changes by 1.5%, 1.6%, and 1.2%, and the bond lengths of Fe-O and P-O only changes by 0.5% and 0.8% on the average, respectively. A previous theoretical investigation by Wolverton *et al.*[12] showed that the volume change of $LiCoO_2$ compared with that of CoO_2 is 14%, and another theoretical value by plane wave pseudopotential method is 10%.[25] Hereby the volume change from $LiFePO_4$ to $FePO_4$ is much smaller. In other words, the structural rearrangement during lithium extraction/reinsertion process in $LiFePO_4$ is very small. This small volume change should be a beneficial factor to achieve a long lifetime for lithium ion battery when $LiFePO_4$ is used as cathode material.

Both Wolverton *et al.*[12] and Aydinol *et al.*[25] proposed that not only Co but also O is oxidized with the removal of Li in $LiCoO_2$. This is at variance with the usual view of the intercalation reaction that the Co ion undergoes the charge change: It changes its oxidation state from Co^{3+} in $LiCoO_2$ to Co^{4+} in CoO_2. In the case of $LiFePO_4$, the same phenomenon is also observed by x-ray photoelectron spectroscopy.[18] For an explanation of the first-principles calculation, Fig. 2 is plotted, which shows the positive part of the difference in

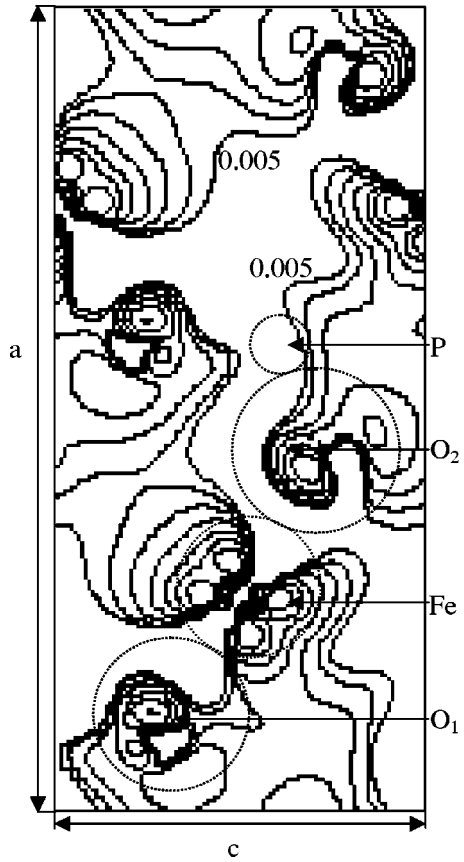

FIG. 2. Calculated isodensity contours of the difference between $LiFePO_4$ and $FePO_4$, $\Delta\rho=\rho[LiFePO_4]-\rho[FePO_4]$, shown on the (010) plane. The contours have densities $\Delta\rho=0.005\times2^n e/$ Å^3, for $n=0,1,2,\ldots,9$. The dashed circles show the ion position and/or the integration radii as discussed in the text. Subscripts of atom symbols correspond to Table I.

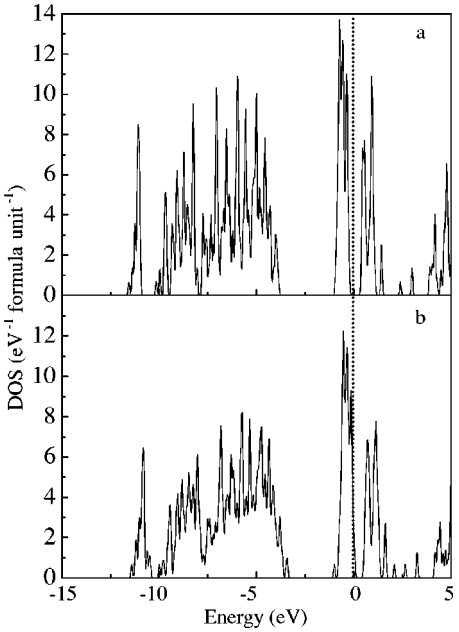

FIG. 3. Total density of states (DOS) of (a) $LiFePO_4$ and (b) $Li_{1-3/32}Cr_{1/32}FePO_4$. The Fermi level is set as a reference.

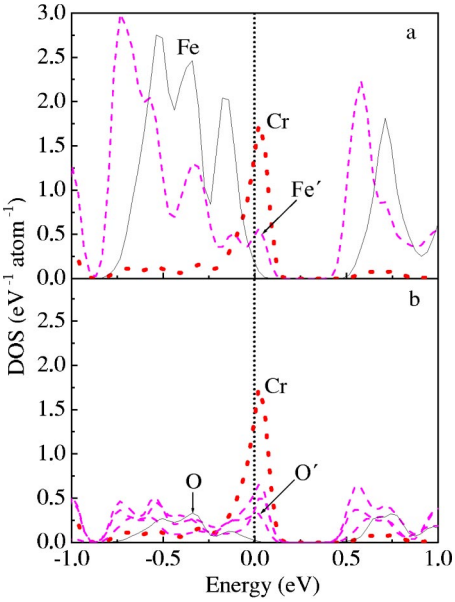

FIG. 4. (Color online) Local density of states of the doped Cr atom and (a) Fe atoms and (b) O atoms in $Li_{1-3/32}Cr_{1/32}FePO_4$. Here, the Fe′ (dashed line) is the Fe atom nearest the Cr atom. O′ (dashed lines) indicates three types of O atoms which are all nearest to Cr, but have different Fe and vacancy neighbors. Solid curves marked by Fe and O are displayed for atoms far from Cr for comparison. The Fermi level is set as a reference.

electron density between $LiFePO_4$ and $FePO_4$ in the (010) plane. Regions of minor electron depletion also exist, but are not shown in this figure. Although the structures given in Table I are fully relaxed, for the theoretical purpose of verifying the difference in this figure, the electron density of $FePO_4$ is calculated at the same lattice parameters and atomic positions as the relaxed $LiFePO_4$, so that the electron densities can be easily subtracted point by point in the real space to show the effect of delithiation. Because lithium is fully ionized in $LiFePO_4$, the difference is only negligible around its position before and after delithiation. From Fig. 2 the *d*-like orbit on Fe and the *p*-like orbit on O_1 and O_2 can be clearly identified. In order to reflect the electron transfer quantitatively, this difference has been integrated around Fe and O, and as the difference of electron density is well localized, it is feasible to integrate it in a sphere around the ions. If we take the integration radii as 0.78 and 1.4 Å for Fe and O, respectively, during the charging process when lithium ions all go away, about 0.14, 0.16, and 0.18 electrons come from O_1, O_2, and Fe atoms, respectively. Meanwhile, Fig. 2 also shows that the delithiation process has little effect on the valence state of P. It is obvious to see that during the delithiation the electron through the external circuit predominantly comes from O, which is even more than that from the transition metal Fe.

Chromium doping needs much more efforts in the computational simulation. Doping model is constructed by a 222-atom supercell, which is generated by firstly doubling the 28-atom orthorhombic $LiFePO_4$ unit cell in all three dimensions, then letting one Li atom be replaced by one Cr atom, and finally putting two vacancies on Li sites around the doping Cr atom. Only one Γ point sampling in the first Brillouin zone was used for this large supercell, which gives approximately the same accuracy in total energy per atom as the 60 *k* points sampling for the 28-atom orthorhombic $LiFePO_4$ unit cell. Other parameters are kept the same as in the case of the pure $LiFePO_4$ (see above). First, we have calculated the total energies of all 45 possible vacancy configurations with the two vacancies on Li sites locating within 6 Å from the doping Cr atom, but we neglect the doping induced structure relaxation. The total energy was found to reach the lowest when the two vacancies are located on both sides of the Cr atom along the *b* direction (see Fig. 1). That is, the configuration in which the two vacancies are nearest to Cr is most favorable in energy, consistent with a Coulombic attraction between the higher valence Cr and the vacancy, which is equivalent to a negative ion on the positive Li ion background. Then, a relaxation calculation is carried out starting from this optimized vacancy configuration, and the structural stability of this configuration is verified. In this relaxation calculation, all ionic positions of this doping model are relaxed with the conjugate gradient method using forces and stresses, but the supercell lattice parameters of the expanded doping model are fixed at the optimized values of pure $LiFePO_4$.

Figure 3 shows the total density of states of $LiFePO_4$ and $Li_{1-3/32}Cr_{1/32}FePO_4$. Pure $LiFePO_4$ is a semiconductor with a gap $\sim$0.53 eV according to this generalized gradient approximation calculation. This is slightly larger than the gap ($\sim$0.3 eV) calculated by Xu *et al.*[26] The narrow band near the Fermi level can be assigned to the 3d band of Fe. The nonbonding t_{2g} states and antibonding e_g states lie in the lower (-1 to -0.11 eV) and higher (0.28–1.5 eV) energy region, respectively. This occupation gives a typical Fe^{2+} state. Comparing with the case of $LiFePO_4$, the Fermi level of $Li_{1-3/32}Cr_{1/32}FePO_4$ lies in the falling edge of the valence

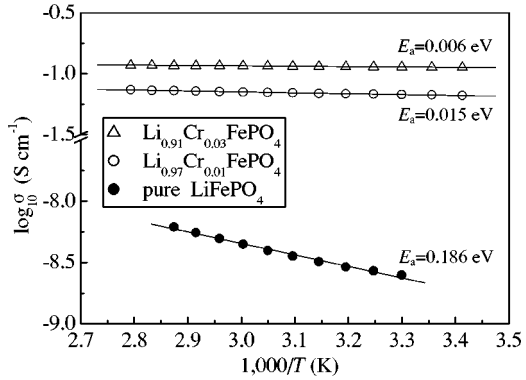

FIG. 5. Electronic conductivity plots for Cr-doped and pure $LiFePO_4$.

band, and thus holes are left at the valence band top. To better compare the difference near the Fermi level, we plot the local density of states of doping-Cr atom, the Fe atom nearest to Cr and all three nonequivalent O atoms which are the nearest to Cr in the energy range from -1 to 1 eV as shown in Fig. 4. It is found that, for $Li_{1-3/32}Cr_{1/32}FePO_4$, electronic states at the Fermi level mainly come from the Cr-$3d$, but contain hybridization with neighboring O-$2p$ and Fe-$3d$ bands of the O and Fe atoms near the dopant.

This Cr-induced state may alter the conductivity with respect to the pure $LiFePO_4$, where no electronic state is located at the Fermi level. Two possible conducting mechanisms could be considered. The first probable mechanism is simple *p*-type conduction by the holes generated at the top of the bulk valence Fe-O bands by the activation of the electrons to the empty impurity Cr states. In fact, Chung *et al.*[6] found that highly conductive doped compositions seem to be extrinsic *p*-type semiconductors. The second probable mechanism is that the complex containing the doped Cr ion, the vacancies on Li sites, and their neighboring Fe and O ions form a conducting cluster. One can notice in Fig. 4 that the localized impurity Cr state crossing the Fermi level has an appreciable hybridization with its neighboring Fe and O atoms. Counting all such atoms, they cover a region over about 21 lattice sites in $LiFePO_4$, including one Cr site, two vacancies, 14 O sites, and four Fe sites. Electronic hopping conduction is feasible within the cluster. This suggests that, for the supervalent metal-doped material, a hopping transport of electrons is also feasible if these doping generated conducting clusters are made dense enough to be percolatively connected through tunneling.

To test the prediction of the calculations we prepare pure and doped samples using the solid-state reaction method. The synthesis procedure is similar to the one proposed by Chung *et al.*[6] Proper amounts of Li_2CO_3, $FeC_2O_4.2H_2O$, $NH_4H_2PO_4$, and Cr_2O_3 corresponding to the ratio of $LiFePO_4$, $Li_{0.97}Cr_{0.01}FePO_4$, and $Li_{0.91}Cr_{0.03}FePO_4$ were mixed by ball milling for 2 h and initial heating to 300 °C in an Ar (92%) + H_2 (8%) atmosphere for 10 h to remove H_2O and NH_3. The resulting product was ground, homogenized, and further heated to 700 °C for 24 h in the same atmosphere and then cooled down to room temperature. X-ray powder diffraction patterns of samples are all in good agreement with standard $LiFePO_4$ (JCPDS 401499) with an ordered olivine structure indexed by orthorhombic *Pnmb*. No obvious evidence of other impurity phases could be detected in this pattern. On the other hand, because the doped Cr^{3+} has an ionic radius smaller in octahedral coordination than that of Fe^{2+},[27] the substitution for Li^+, as described in the present theoretical model, is preferred.

The dc electrical conductivity was measured by a direct volt-ampere method on disk samples prepared by pressing the powder up to 20 MPa, which ensures that the conductivity reaches a stable value. Its diameter and thickness are 1.3 cm and 1 mm, respectively. In Fig. 5, it can be clearly seen that doped $Li_{0.97}Cr_{0.01}FePO_4$ and $Li_{0.91}Cr_{0.03}FePO_4$ show an electronic conductivity $\sim 10^8$ greater than that of pure $LiFePO_4$ at room temperature.

It is interesting to note that the activation energy $E_a = 0.186$ eV of pure $LiFePO_4$ approximates one half of the calculated gap E_g (~ 0.53 eV), indicating that pure $LiFePO_4$ is an intrinsic semiconductor. On the other hand, from Fig. 5, we can also see that the doping leads to an obvious decrease of the activation energy to 0.006–0.015 eV. Calculated E_F of the Cr-doped $LiFePO_4$ is about 0.04 eV above the bulk valence band top. So a *p*-type conduction is feasible with an activation energy about 0.02 eV. However, the present activation energy of pure $LiFePO_4$ is smaller than the one (~ 0.5 eV) given by Chung *et al.*,[6] and the activation energy of the present Cr-doped sample is much smaller than Mg-, Zr-, and Nb-doped samples.[6] This may be ascribed to some unknown difference in the preparing process.

Though the simple *p*-type doping conduction mechanism explains the existing conductivity data fairly well, we should also point out that there is another possibility. For $Li_{1-3x}Cr_xFePO_4$, if we assume that the conducting cluster around each Cr atom consists of about 21 lattice sites, the volume ratio of such a cluster accounts for about 3% and 9% of the total volume when $x = 0.01$ and 0.03, respectively. At this volume ratio, the conducting cluster might be percolatively connected, either directly or through tunneling. The nearly vanishing activation energy in $Li_{0.91}Cr_{0.03}FePO_4$ might be, at least partly, due to this additional contribution.

This work was supported by the National Science Foundation of China (NSFC) (No. 50272080), National 973 program (2002CB211802) and National 863 key programs (2001AA32301) and (715-004-0280). D.W. was supported by Pan-deng Project (No. G19990328-2).

[1] G. Ceder, Y.-M. Chiang, D.R. Sadoway, M.K. Aydinol, Y.-I. Jang, and B. Huang, Nature (London) **392**, 694 (1998).
[2] J. Kim and A. Manthiram, Nature (London) **390**, 265 (1997).
[3] J.-M. Tarascon and M. Armand, Nature (London) **414**, 359 (2001).
[4] H. Shimoda, B. Gao, X.P. Tang, A. Kleinhammes, L. Fleming, Y. Wu, and O. Zhou, Phys. Rev. Lett. **88**, 015502 (2002).
[5] M. Winter, J.O. Besenhard, M.E. Spahr, and P. Novak, Adv.

Mater. (Weinheim, Ger.) **10**, 725 (1998).
[6] S.-Y. Chung, J.T. Bloking, and Y.-M. Chiang, Nature Mater. **1**, 123 (2002).
[7] A. Manthiram and J.B. Goodenough, J. Power Sources **26**, 403 (1989).
[8] A.S. Andersson and J.O. Thomas, J. Power Sources **97-98**, 498 (2001).
[9] Atsuo Yamada, Yoshihiro Kudo, and Kuang-Yu Liu, J. Electrochem. Soc. **148**, A747 (2001).
[10] H. Huang, S.-C. Yin, and L.F. Nazar, Electrochem. Solid-State Lett. **4**, A170 (2001).
[11] M. Thackeray, Nature Mater. **1**, 81 (2002).
[12] C. Wolverton and A. Zunger, Phys. Rev. Lett. **81**, 606 (1998).
[13] C. Wolverton and A. Zunger, Phys. Rev. B **57**, 2242 (1998).
[14] V. Meunier, J. Kephart, C. Roland, and J. Bernholc, Phys. Rev. Lett. **88**, 075506 (2002).
[15] M.V. Koudriachova, N.M. Harrison, and S.W. de Leeuw, Phys. Rev. Lett. **86**, 1275 (2001).
[16] Siqi Shi, Ding-sheng Wang, Sheng Meng, Liquan Chen, and Xuejie Huang, Phys. Rev. B **67**, 115130 (2003).
[17] J. Zhao, A. Buldurn, J. Han, and J.P. Lu, Phys. Rev. Lett. **85**, 1706 (2000).
[18] Lijun Liu, Siqi Shi, Zhaoxiang Wang, Liquan Chen, and Xuejie Huang (unpublished).
[19] Aintzane Goñi, Luis Lezama, Ainhoa Pujana, Maria Isabel Arriortua, and Teofilo Rojo, Int. J. Inorganic Mat. **3**, 937 (2001).
[20] G. Kresse and J. Hafner, Phys. Rev. B **47**, 558 (1993); **49**, 14251 (1994); J. Phys.: Condens. Matter **6**, 8245 (1994); G. Kresse and J. Furthmüller, Comput. Mater. Sci. **6**, 15 (1996); Phys. Rev. B **54**, 11169 (1996).
[21] D. Vanderbilt, Phys. Rev. B **41**, 7892 (1990).
[22] J.P. Perdew, J.A. Chevary, S.H. Vosko, K.A. Jackson, M.R. Pederson, D.J. Singh, and C. Fiolhais, Phys. Rev. B **46**, 6671 (1992).
[23] M. Methfessel and A.T. Paxton, Phys. Rev. B **40**, 3616 (1989).
[24] V. Streltsov, E.L. Belokoneva, V.G. Tsirelson, and N.K. Hansen, Acta Crystallogr., Sect. B: Struct. Sci. **49**, 147 (1993).
[25] M.K. Aydinol, A.F. Kohan, G. Ceder, K. Cho, and J. Joannopoulos, Phys. Rev. B **56**, 1354 (1997).
[26] Y.-N. Xu, W.Y. Ching, S.-Y. Chung, J.T. Bloking, and Y.-M. Chiang (unpublished), as cited in Ref. 6.
[27] R.D. Shannon, Acta Crystallogr. Sect. A: Cryst. Phys., Diffr., Theor. Gen. Crystallogr. **32**, 751 (1976).